

Preparation of C-fibre borosilicate glass composites: Influence of the fibre type on mechanical properties

T. KLUG, R. BRÜCKNER

Institut für Nichtmetallische Werkstoffe, TU Berlin, Germany

Nine different types of carbon fibres were used as the reinforcement component of the borosilicate glass DURAN. Optimum preparation procedures and parameters for the resulting composites were investigated, the mechanical properties were measured in the bending test, and the results compared. It was found that the densification of composites incorporated with high-modulus (hm) C-fibres could be done at lower temperatures than that of composites with high-strength (hs) C-fibres. The utilization of the fibres in the composites with respect to the tensile strength of the fibres was much better for the hm-C-fibres than for the hs-C-fibres. The experimentally obtained values for Young's modulus and the bending strength of the composites were compared with those calculated from the linear mixing rule (LMR). The measured bendover stresses (stress limit of the elastic region in the stress–strain diagrams) were compared with those from the Aveston–Cooper–Kelly model, which calculates stresses at which cracks in the glass matrix occur. It has been shown that good agreement between experimental and calculated values was found if relatively large values were assumed for the interfacial shear strength.

1. Introduction and objective

During the last two decades it has been reported in many papers, e.g. [1, 2], that the low strength and high brittleness of inorganic glasses can be improved drastically by long C- and SiC-fibre reinforcement either uni- and bidirectionally. In addition, excellent properties were obtained, such as thermal shock resistance [3], friction and wear behaviour [4, 5], and hardness.

The goal of the present investigation was to find out the optimum preparation conditions of C-fibre/glass composites. Of special interest was the influence of the various types of commercially available C-fibres. The largest enhancement of strength and toughness were obtained by reinforcement with long continuous fibres [6]. Therefore only infinite fibres were used.

Carbon fibres were received as fibre bundles with 1000–16 000 single filaments, woven as textile and felt [7]. The preparation was done by thermal decomposition of selected organic fibres, e.g. cellulose, pitch, polyacrylonitrile (PAN) or other long-chain organic compounds [1, 7, 8]. Most reliable fibres were produced from PAN-precursors, in a two step process:

1. The PAN-fibres were heated to 250 °C while the fibre was kept under small tension. This led to degassing and chemical connection reactions, and to a transition into a non-melting form in which cross-linking was eliminated. Simultaneously the colour changed from white to black.
2. The fibres were heated to temperatures between 1200 and 1600 °C in an inert atmosphere and were

transferred into carbon fibres in which all other elements were nearly eliminated.

The tensile strength of the fibres had a maximum at a preparation temperature of ca. 1400 °C [2]. Fibres heated up to 1600 °C are called high-strength (hs) fibres. These fibres could be structurally ordered to a high degree by a heat treatment at 3000 °C. This process of graphitizing and recrystallizing with simultaneous mechanical stretching changed the hs-fibres to hm-fibres in which no gas was left. All carbon fibres were anisotropic and were built up in their crystalline fine structure and bondings by the graphite modification [9] – strong σ -bonds in the hexagonal layer and weak π -bonds perpendicular to it. The hm- and hs-fibres differed in the degree of crystal order. While the hm-fibres were well ordered (long-range order), the hs-fibres were less ordered [8]. This led to a better chemical resistance and to a larger Young's modulus in the hm-fibres [7]. With respect to the structural model, the C-fibres were built-up by band-like crystallites 6 nm wide and > 100 nm in length [7], which were oriented in the direction of the fibre axis. These crystalline bands gathered to form microfibrils.

Hs-fibres contained a final content of 2–7 wt % nitrogen [7, 10, 11] due to their low temperature treatment. The release of nitrogen became significant from 750 °C, connected to the fracture of C–N-bonds and to recombination of nitrogen gas diffusing out of the fibres. This release had the consequence of degradation of the fibre strength with the treatment at high

temperatures. Increasing the nitrogen concentration of the fibres diminished the oxidation resistance. In addition to nitrogen, hydrogen could also be present up to 0.5 wt % in hs-fibres. Hm-fibres were free from both components.

The Young's moduli of commercially produced hs-fibres are 200–300 GPa and the tensile strength between 4000 and 7000 MPa. The values for hm-fibres are 300–700 GPa and 2000–4000 MPa, respectively [12]. The Young's modulus could be increased slightly by increasing fibre strain to between 1 and 2% for hs-fibres and 0.5–1% for hm-fibres. Very large Young's moduli were obtained for fibres prepared from pitch-prefibres [13]. The Young's moduli were much smaller in the radial direction due to the anisotropy of their bonding and orientation [14]. The anisotropy of the crystalline structure and bonding lead to a slightly negative thermal expansion coefficient in the hexagonal layer and in fibre direction ($\alpha_{-200;350} = -0.51 \times 10^{-6} \text{ K}^{-1}$ or $\alpha_{20-1000} = 1 \times 10^{-6} \text{ K}^{-1}$, respectively) and to a very large one perpendicular to it ($\alpha_{20-1000} = 30 \times 10^{-6} \text{ K}^{-1}$) [15].

Carbon fibres have a low fatigue and a large creep resistance in the fibre axis direction. Therefore, C-fibre reinforced materials show a high long-time strength under alternating bending and tensile load [16]. The only disadvantage is the low oxidation resistance of the C-fibres above 400–500 °C. Under vacuum, or in an inert gas atmosphere, the hm-C-fibres can be heat-treated up to > 2500 °C without a decrease in strength [10].

2. Experimental procedure

Composites were prepared by the sol-gel slurry method [17, 18]. A silicon alkoxide solution was used instead of the usual suspension solution, with an organic binder on wax to impregnate and "glue" the glass powder to the fibre bundles.

DURAN glass, a borosilicate glass (Schott Glaswerke, Mainz) was used as the glass matrix. It was shown in previous investigations [19] that a fine-grain size glass powder (mean size < 5 µm) resulted in a homogeneous fibre distribution with enhanced mechanical properties.

The fibre bundles were impregnated by drawing them through a swirl bath slurry with air blown from

below. The fibre volume content of the composites was regulated exactly by the ratio of glass powder: alkoxide solution. After impregnation the fibre bundles were wound parallel on a drum which was hexagonal in cross-section, to a total thickness of ca. 25 fibre bundle layers.

After several drying steps the hexagonal prepreg body was taken from the drum and sawn into six quadratic prepreg plates, $10 \times 10 \times 1.5 \text{ cm}^3$. The densification of the prepreps was done by hot pressing. Further details are given in [17–19].

PAN-carbon fibres (Torayca, Japan) were used as the reinforcement component. The fibre supplied by this company is divided in three series [12]; fibres from the T-series are characterized by a high tensile strength and by an intermediate Young's modulus, the M-series by a low tensile strength and a large Young's modulus and the MJ-series by a relatively high tensile strength and a large Young's modulus. Table I contains some characteristic properties of the fibres used (producer's data) and Fig. 1a and b show SEM micrographs of T800HB and of M55J fibres, respectively.

Three-point bending tests served as a control and characterization of the mechanical properties. For this reason the composite plates were cut into rods of $95 \times 3 \times 4 \text{ mm}^3$ (length \times height \times width) by a diamond saw. The span of the bending test set-up was 75 mm in order to guarantee neglect of the influence of the always present shear component by keeping the ratio $l/h > 20$ [20, 21] (l = span width, h = sample height). The samples were placed in the test device so that the load and the hot-pressing direction were parallel. The experiments were performed with a universal test machine from Zwick (type 1455) at a constant strain rate of 10 mm min^{-1} . The strains were measured with the help of an inductive differential transformer. The bendover stress and strain values, which indicate the region of the pure linear elastic regions of the composites, were determined from the stress-strain diagrams, as were the bending stress and the strain values of the maximum fracture stress.

The bendover stress is a result of the initial damage of the glass matrix due to multiple crack formation. It is the upper load limit in the practical use of a composite below which no damage or fatigue effects occur [16]. With the onset of crack formation in the matrix above this limit the fibres are no longer

TABLE I Characteristic properties of various types of C-fibres (producer's data)

| Fibre | Tensile stress (MPa) | Young's modulus (GPa) | Strain at max. fracture stress (%) | Density (g cm^{-3}) | Fibre diameter (μm) | Axial thermal expansion coefficient 10^{-6} K^{-1} |
|-------|----------------------|-----------------------|------------------------------------|--------------------------------|----------------------------------|--|
| T300 | 3530 | 230 | 1.5 | 1.76 | 7 | 0.3 |
| T800 | 5490 | 294 | 1.9 | 1.81 | 5 | 0.1 |
| T1000 | 7060 | 294 | 2.4 | 1.82 | 5 | 0.1 |
| M40J | 4410 | 377 | 1.2 | 1.77 | 6 | 0 |
| M46J | 4210 | 436 | 1.0 | 1.84 | 5 | - 0.7 |
| M55J | 3920 | 540 | 0.7 | 1.93 | 5 | - |
| M60J | 3920 | 588 | 0.7 | 1.94 | 4.7 | - 0.9 |
| M30 | 3920 | 294 | 1.3 | 1.70 | 6.5 | - |
| M40 | 2740 | 392 | 0.6 | 1.81 | 6.5 | - 1.2 |

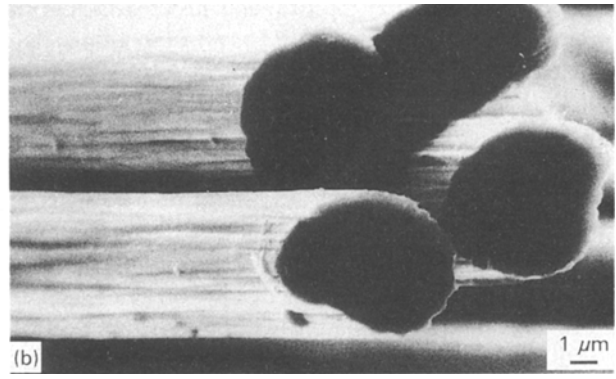
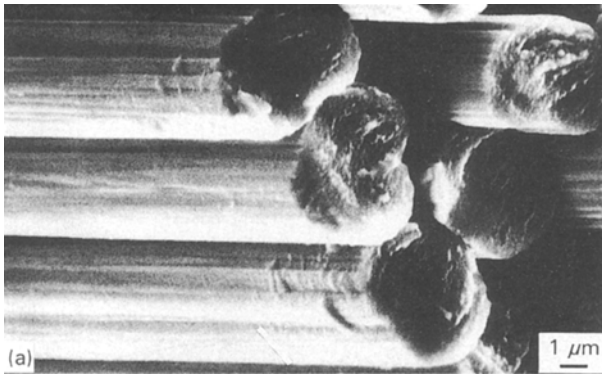


Figure 1 SEM micrographs of carbon fibres from type T800HB (a) and M55J (b).

protected by the glass matrix and influence of the environment becomes possible [22].

The fibre volume concentration of the composites was determined and controlled by a microscope combined with a video camera and an analyser (type 40-10 from A. J. Tektron) which digitized the image of the polished cross-section of the composite in 256 grey steps. With the election of one of these steps as a threshold value it was possible to automatically count the volume fraction of those objects for which the grey step was above the threshold value. The different reflexivity of the reflected light from fibre and matrix was used by this method. By means of the choice of the objective and by regulation of the analyser a circular area of 80 μm diameter of the composite was analysed. Twenty single determinations over the cross-section of a composite were performed to determine the mean value of the fibre volume concentration. The error was ± 2 vol %.

The density was determined by the Archimedes method with an error of $\pm 0.02 \text{ g cm}^{-3}$.

3. Results

3.1. Influence of pressing temperature on the mechanical properties of hs-C-fibre/DURAN glass composites

The bending strength, bendover stress and the corresponding strains are plotted versus pressing temperature in Fig. 2a and b, respectively. The fibre content was 40 ± 2 vol %, the final pressure was 7 MPa (the optimum one after [19]). Maxima were found for the strength and strain at maximum fracture stress at 1250

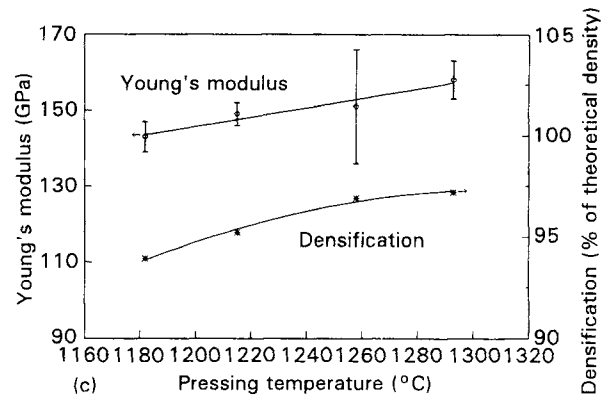
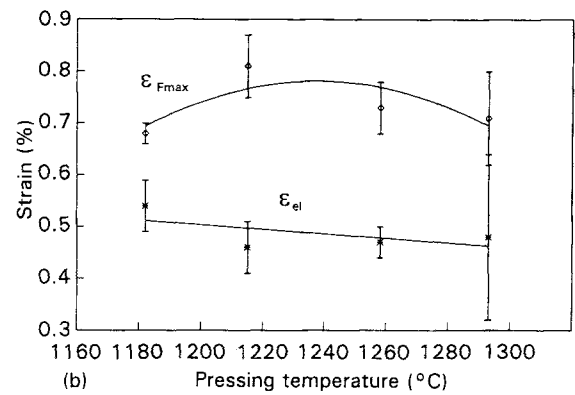
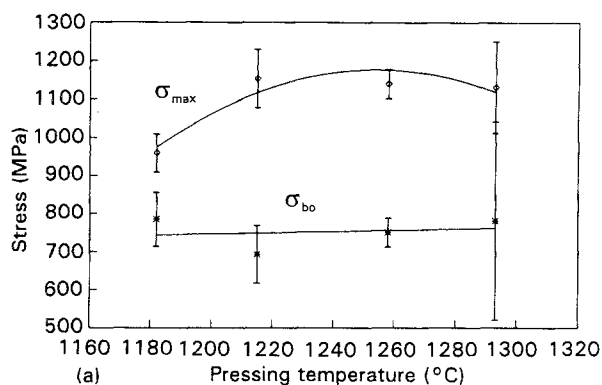


Figure 2 Mechanical properties versus pressing temperature for composites C-fibre T800/DURAN glass with fibre content $V_f = 40$ vol %. (a) Bending strength (σ_{max}) and bendover stress (σ_{bo}); (b) strains at maximum stress (ϵ_{Fmax}) and at bendover stress (ϵ_{bo}); (c) Young's modulus and densification (% of theoretical density).

to 1260 °C. In contrast, the bendover stress and strain values were constant over the same temperature range. High pressing temperatures caused an increase in the scattering range of the measurements, indicating the beginning of fibre degradation and a disturbance of the fibre architecture of the composites.

Young's modulus (Fig. 2c) increased with increasing pressing temperature having the value of 155 GPa, in exact agreement with the value calculated by the linear mixing rule (LMR). The densification of the composites also increased with temperature (Fig. 2c).

The C-fibre T800 contained as a typical hs-fibre a certain "rest" amount of nitrogen, which was released during hot pressing. Additionally, the fibre had a very

rough surface due to the drawing process during its preparation (see Fig. 1a). Both facts lead to an increase in densification of the composites with increasing pressing temperature (Fig. 2c): the release of nitrogen from the fibre decreased at higher temperatures as did the viscosity of the glass melt resulting in an easier escape of nitrogen on the one hand and in a better penetration of the melt into the fine surface roughness of the fibres on the other. The reason why Young's modulus increased was also due to the increasingly close fibre-matrix contact. It will be shown in Section 3.2 that there were no pores or clusters if nitrogen-free hm-fibres were used for reinforcing the DURAN-glass.

Fig. 3 shows a large survey of the microstructure of a typical composite C-fibre T800/DURAN glass. The fibres are oriented perpendicular to the cross-section and distributed inhomogeneously. There are fibre-poor and fibre-rich clusters and pores, the latter ones being due to the nitrogen release [7, 10, 11].

The use of higher pressing temperatures lead increasingly to the pressing out of glass melt from the pressure cell, and therefore to an alteration of the fibre concentration and to a disturbance of the unidirectional orientation of the fibres. Additionally, the T800-fibre degraded with increasing temperatures, thus, the application of higher pressing temperatures was not meaningful for these composites. The optimum hot-pressing parameters of this system (T800/DURAN) were also used for other investigated systems, T300/DURAN and T1000/DURAN, for which characteristic values are given in Tables I-III.

3.2 Pressing temperatures and mechanical properties of hm-C-fibres/DURAN glass composites

The influence of pressing temperature on the mechanical properties of the system C-fibres M55J/DURAN glass is described, also representing the behaviour of other hm-C-fibre/DURAN glass systems. Fig. 4 represents the results of bending experiments of the composites with a fibre content of 40 vol % which were densified at a pressure of 7 MPa as a function of pressing temperature. Bending strength and bendover

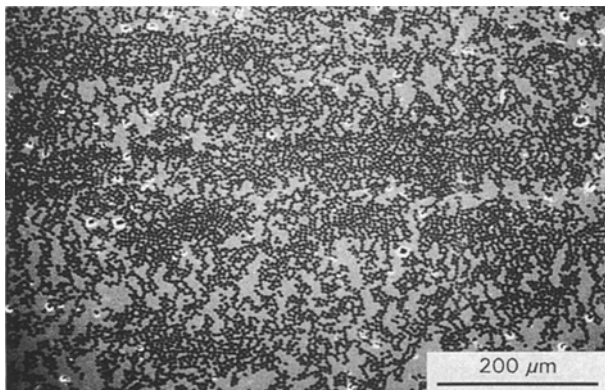


Figure 3 Microstructure (SEM) of a composite C-fibre T800/DURAN glass with $V_f = 40$ vol %.

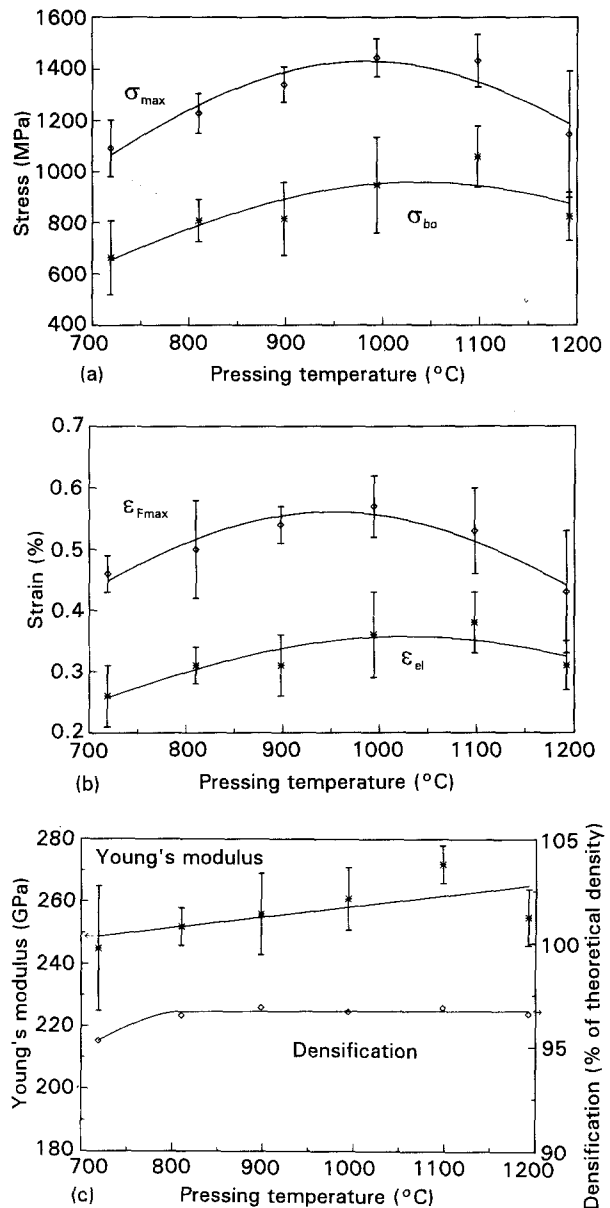


Figure 4 Mechanical properties versus pressing temperature of composites C-fibre M55J/DURAN glass with $V_f = 40$ vol %. (a) Bending strength (σ_{max}) and bendover stress (σ_{bo}); (b) strains at maximum stress (ϵ_{Fmax}) and at bendover stress (ϵ_{bo}); (c) Young's modulus and densification.

stress show maxima at 1000–1100 °C. Large values for the strength and for the corresponding strain are found at relatively low pressing temperatures (Fig. 4b); a composite densified at 800 °C had only slightly lower values for the bending strength and bendover stress than a composite which was densified at much higher temperatures. For comparison: hs-C-fibre T800/DURAN glass composites showed optimum values only > 1200 °C (Section 3.1).

The reason for this different densification behaviour is that the hm-C-fibres are free of nitrogen and do not cause porosity of the glass matrix at low pressing temperatures, and the hm-C-fibres are better wetted by the glass melt than the hs-fibres [10]. Fig. 4c shows that the densification at 720 °C was only slightly lower than that at the other pressing temperatures.

At such low temperatures necessary for pressing the hm-C-fibre/DURAN glass composites the danger of crystallization exists. Fig. 5 indicates that the

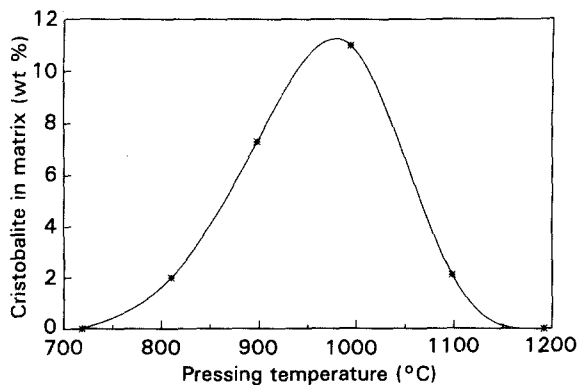


Figure 5 Formation of cristobalite in wt % in the DURAN glass matrix at low pressing temperatures; system M55J/DURAN, $V_f = 40$ vol %; pressing time 5 min.

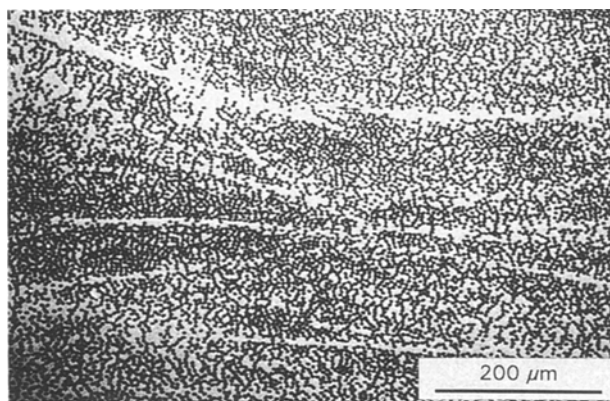


Figure 6 Microstructure of a composite C-fibre M55J/DURAN glass; $V_f = 40$ vol %.

DURAN glass matrix devitrifies slightly to cristobalite at low pressing temperatures (750–1100 °C) up to an amount of ca. 10 wt % (determined by X-ray diffraction). The thermal expansion mismatch between the cristobalite crystals and the surrounding DURAN glass matrix, as well as the high–low temperature transition of cristobalite at 230 °C, can lead to a slight degradation of those composites which were densified between 800 and 1000 °C.

Fig. 6 gives an impression of the microstructure of hm-fibre M55J/DURAN composite densified at 1100 °C. Although the single layers of fibre bundles are visible, a good homogeneous fibre distribution with no cluster formation was observed, in contrast to the hs-fibre/DURAN glass composites. The better wettability of the hm-C-fibres implies a lower separation tendency of fibres and matrix, whereas the lower wettability of the hs-C-fibres implies a stronger one and leads to inhomogeneities and cluster formation (Fig. 3).

A comparison between stress–strain diagrams of composites reinforced by hm- and hs-C-fibres is given in Fig. 7. The fracture behaviour of these composites is a brittle one for 40 vol % fibre content. One reason for the low toughness in the bending test is the relatively large shear strength of these composites (ca. 70 MPa for system T800/DURAN and ca. 90 MPa for system M55J/DURAN from short-beam bending tests). The

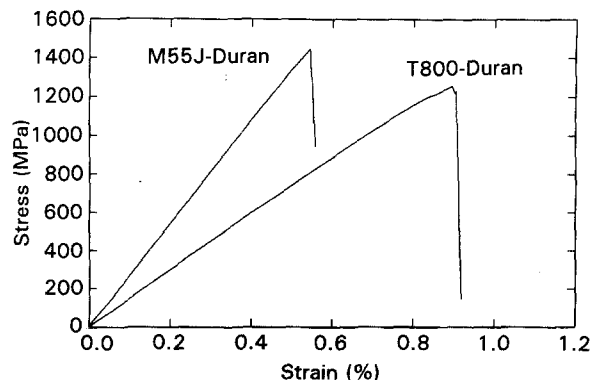


Figure 7 Stress–strain diagrams of composites from system M55J/DURAN and system T800/DURAN; $V_f = 40$ vol %.

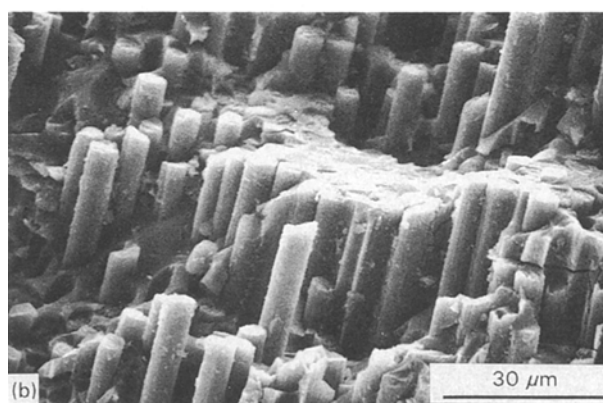
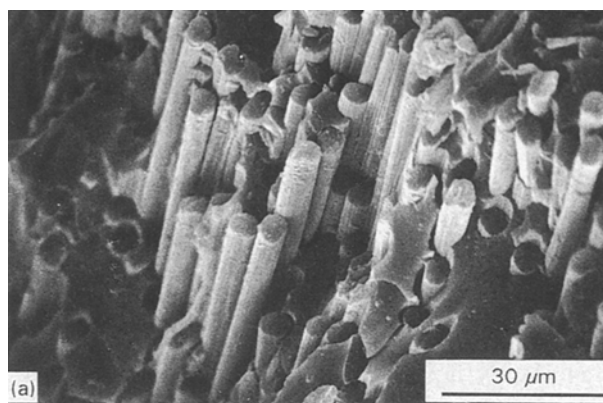


Figure 8 Fracture surface at the tensile stress side of composites in a beam bending test; $V_f = 40$ vol %. (a) system T800/DURAN; (b) system M55J/DURAN.

large interlaminar shear strength also indicates a large interfacial shear strength by which delamination processes and crack branching are reduced. In another investigation it was shown that a fibre volume content of ca. 50 vol % lead to high toughness of the composites [19], also true for hm-fibre reinforced glass with 50 vol % fibre content. Fig. 8 shows SEM micrographs of fracture surfaces from the tensile side of bent hm-C- and hs-C-composites with 40 vol % fibre content. It is obvious that many fibres were cut by cracks directly at the same level of the fracture surface as the matrix. Only a few fibres were seen to be free and from those no fibres seemed to be pulled out, i.e. the extent of crack branching was small. An indication that no pull-out effect of fibres occurred is that no holes from

broken fibres within the glass matrix were observed. Those fibres seen in Fig. 8 are free from the matrix because the matrix had simply broken away from the fibres during the crack propagation. Therefore, cracks were deflected parallel to the fibres at the tensile side of a bent sample after exceeding the tensile strength of the fibres; but those cracks were deflected only to a very low degree. Thus, no effective crack stop occurred and the sample was divided into two parts parallel to the fibres before the normal stress could increase within the still unbroken part of the sample.

The better the order of the graphite layers of a fibre, the more susceptible the fibre is to longitudinal shear [23]. Therefore, the probability that a matrix crack, reaching a fibre, will cut this fibre directly or after a short deflection, is larger for hm-fibres than for hs-fibres. The consequence of that is a smaller effect of delamination and, thus, of resulting lower toughness in the bending test for hm-fibre than for hs-fibre reinforced composites.

All DURAN glass composites reinforced by other hm-C-fibres of the MJ- and M-series were prepared at 1100 °C with a final pressure of 7 MPa. (Characteristic values are given in Tables II and III).

4. Discussion

4.1 Influence of pressing temperature

Significantly higher pressing temperatures are needed for the densification of glass composites reinforced by hs-C-fibres than for hm-C-fibres (cf. Figs 2 with 3). Pressing temperatures < 1200 °C for the former ones lead to poor mechanical properties due to porosity. The origin of the porosity at low pressing temperatures was due to the high nitrogen content of the hs-C-fibres, which was up to 4 wt % N₂ for T800-fibres [11] and up to 7 wt % N₂ for T300-fibres [10]. The greatest influence of the pressing temperature on the mechanical properties and on the densification was measured for composites with this fibre type (T300). The release of nitrogen from the T300-fibres became significant ≥ 750 °C [10]. The large decrease of porosity of the corresponding composites in these experiments indicate that the N₂-release was almost complete at 1200 °C.

Composites reinforced with hm-fibres were densified to the same amount above 800 °C and had large strength values (Fig. 4). However, a slight devitrification of the glass matrix appeared at low pressing temperatures (800–1000 °C) with a maximum crystal content at 950 °C (Fig. 5). The crystal phase was cristobalite, with an amount at 950 °C pressing temperature of 10 wt % relative to the glass matrix. The crystal growth rate maximum at 950 °C was confirmed in [24, 25], where the system SiC-fibre/PYREX glass was investigated and a quantity of 18–48 wt % cristobalite was obtained depending on the pressing time. The thermal expansion mismatch by the different expansion coefficients and by the transition from the high to the low temperature modification of cristobalite at 230 °C originated crack formation and therefore reduced mechanical properties. Low amounts of cristobalite did not influence the properties. No cristo-

balite was observed at pressing temperatures > 1077 °C [26].

The variation of the pressing temperature for the various fibre/DURAN glass systems was extended up to temperature at which large amounts of glass melt were pressed out of the pressure cell. This caused a flow and disturbed the (unidirectionally) orientation of the fibres, the fibre volume concentration was altered in an uncontrolled manner. It cannot be excluded that chemical reactions between fibres and the borosilicate matrix may also occur at very high pressing temperatures, which may lead to fibre degradation.

4.2 Application of the linear mixing rule (LMR) on Young's modulus and bending strength

The LMR is usually suitable primarily to calculate or to estimate the density and Young's modulus of composite materials. Within a certain stress range linearity is found between stress and strain and the components of the composite remain unchanged under stresses within this range. Restrictions of the validity of the LMR [27] may arise from internal structural specialities with respect to the present investigation, such as thermal stresses due to thermal expansion mismatch and undefined boundings between fibres and matrix via adhesion effect, rough interfaces, etc.

Young's modulus is calculated by the LMR using:

$$E_c = E_m V_m + E_f V_f \quad (1)$$

where E is Young's modulus, V is the portion of volume, c is composite, m matrix and f fibre.

The LMR can also be used to provide a rough estimate of the bending strength when the failure of the samples is initiated by the fibres at the tensile side in the bending test. Because of the fact that the matrix is already damaged by microcracks at this stage, the LMR is reduced to the portion of the fibres only:

$$\sigma_c = \sigma_f V_f \quad (2)$$

where σ_c is the strength of the composite and σ_f is the strength of fibre. This presupposes that the fracture occurs in the bending test on the tensile stress side of the composite.

Table II compares the experimental values with the calculated values after the LMR. All composites were produced under optimum conditions (see Section 3.1 for hs-C-fibre composites and Section 3.2 for hm-C-fibre composites). Young's moduli of both series correspond well to each other. The deviations are smaller than 10% and are due to errors of measurement, such as small errors for fibre concentration determination ± 2 vol % or slightly inhomogeneous fibre distributions.

Good agreement between experimental and theoretical values for the bending strength were obtained from some hm-C-fibre/DURAN glass composites. This indicates a good utilization of these fibres. Poor agreement was found for the hs-C-fibre/DURAN glass composites. Obviously, the decrease of strength due to the nitrogen release of these fibres and their degrada-

TABLE II Bending strength and Young's modulus of various C-fibre/DURAN glass composites ($V_f = 40$ vol %) and calculated values from LMR according to Equations 1 and 2 (%)

| Fibre | Composite, σ_{\max} (MPa) | LMR (2) (%) | Composite, Young's modulus (GPa) | LMR (1) (%) |
|-------|----------------------------------|-------------|----------------------------------|-------------|
| T300 | 684 ± 43 | 48.4 | 137 ± 5 | 105.5 |
| T800 | 1177 ± 52 | 53.6 | 152 ± 10 | 97.8 |
| T1000 | 1249 ± 34 | 44.2 | 161 ± 5 | 103.6 |
| M40J | 1173 ± 100 | 66.5 | 180 ± 5 | 95.4 |
| M46J | 1589 ± 135 | 94.4 | 211 ± 13 | 99.4 |
| M55J | 1434 ± 101 | 91.5 | 272 ± 6 | 107.2 |
| M60J | 1647 ± 80 | 105.0 | 278 ± 6 | 101.8 |
| M30 | 1085 ± 63 | 69.2 | 153 ± 6 | 98.5 |
| M40 | 1182 ± 60 | 107.8 | 210 ± 7 | 107.9 |

tion, as well as pore formation, play an important role. In [11] it was found that the strength of the C-fibre T800 degraded after heat treatment in argon at a temperature of 800 °C, and degraded after 30 min treatment at 1200 °C to a value corresponding to the strength of the hm-fibre M40. This effect explains the bad utilization of the hs-fibres, because the strength values of the composites with 40 vol % M40- and 40 vol % T800 fibres agree well with each other.

It seems that for a good utilization of the strength of fibres the tensile strength: Young's modulus ratio of the fibres should be low (Table II). A low ratio has the consequence that the strain of the composites at the tensile strength of the fibres is relatively small. By this means the crack openings of the multiple matrix cracks remain small and the relative movement (sliding) between fibre and matrix, required for the opening of cracks, takes place only to a small extent. This relative movement can be disadvantageous for the fibres because they can be damaged by the friction of the fragments of the broken matrix. The hm-fibres M40J and M30 have a middle tensile strength: Young's modulus ratio, therefore, their tensile strength can be utilized only up to certain degree. It may be argued that this effect is superimposed by the fibre degradation due to the nitrogen release in the case of the hs-fibres.

In [28] it is reported that the bending strength of hm-C-fibres/PYREX glass composites agree well with the LMR when the fibre content does not exceed 40 vol %. In further investigations [29], considerations about Young's modulus with the LMR resulted in the conclusion that the utilization of C-fibres (obtained from Process Technology Division at AERE) in PYREX glass composites is ca. 80–95%.

4.3 Calculation of the bendover stress

Concerning the work of Aveston, Cooper and Kelly (ACK) [30] there exists a critical fibre volume concentration in composites at which the first crack in the matrix, produced by an outer load, does not lead to fracture of the whole composite. At fibre concentrations beyond this critical value the fibres can take over the additional load, in the course of which multiple

crack formation in the matrix occurs with further loading.

With the help of the equation of ACK a critical fibre concentration of 1.2 vol % is calculated for the system T800/DURAN glass. It can be assumed therefore, that for all composites in the present investigation the fibre volume content was large enough to ensure that multiple crack formation took place. It may be remarked that it was impossible to make these cracks visible under light microscope or in SEM after deloading. Obviously, they were closed again by fibres bridging over the cracks and/or by undamaged matrix regions at deloading of the composites. Only under tensile stress are these multiple cracks visible [31], but this was not done in the present investigation. However, the beginning of damage to the matrix was measured by determination of the limit of the strict proportionality (Hookian range) in the stress–strain diagrams of bended composites, the so-called bendover stress and strain.

The key of the model for the multiple crack formation after ACK is an energetical presupposition [30] in which the strain at fracture of the matrix in composites is always larger than that of the unreinforced matrix. The strain at fracture is reached when the outer forces and the decrease of the elastically stored energy in the matrix is larger than the sum of energies which are necessary to create the fracture surfaces, the debonding of the fibres, the work of friction when the matrix is sliding relative to the fibres and the increase of the elastic energy of the fibres. Under the assumption of chemically unbonded interfaces, i.e. only adhesion and friction is acting, the following relation is found for the strain at fracture of the matrix:

$$\varepsilon_0 = [12 \tau_i \gamma_m E_f V_f / (E_c E_m r V_m)]^{1/3} \quad (3)$$

where ε_0 is the strain at matrix fracture, τ_i the interfacial shear strength, γ_m the surface energy of the matrix and r the fibre radius.

The connection between the strain at matrix fracture, ε_0 , and matrix strength, σ_0 , is given by Young's modulus of the composite, i.e. $\sigma_0 = \varepsilon_0 E_c$.

In another paper the authors ACK distinguished between unbonded (only by friction fixed fibres) and chemically bonded fibres [32]. No significant difference for the strain at matrix fracture was found.

The question about the bonding condition of C-fibres in a glass matrix cannot be answered without some assumptions. The radial thermal expansion coefficient of the C-fibres is many times larger than that of the glass matrix; for the hs-C-T800 fibre it is $26.8 \times 10^{-6} \text{ K}^{-1}$ within a temperature range of 20–500 °C [15], while that of DURAN glass is $3.37 \times 10^{-6} \text{ K}^{-1}$ in the same temperature range. If the C-fibre were to "shrink off" the glass matrix below the glass transition temperature (T_g) of the DURAN glass a gap of 0.06 μm width would be the numeric result; and if the theory of Hegeler and Brückner [33] were true gaps of 0.12 μm should be found. However, no such gap was observed by SEM in these experiments, or those reported in [34]. Therefore, it is now assumed that an intensive adhesion by mechanical keying is produced at the pressing temperature because the surface of the

C-fibres is rough and the interfacial shear strength can vary during the failure of the composite [35]. An increase of the fracture (toughness) resistance of the fibre-matrix interface was observed with increasing roughness of the C-fibre surface [36].

With a certain restriction, it may be said that pure tensile stress is the basis of the ACK model, its application to the bending test may therefore be based on the assumption that the crack formation in the matrix is also produced by tensile stresses. Also assumed is a homogeneous, ideal fibre distribution. These experiments have shown that ideal conditions are rarely found. For the application of the ACK model the amount of the interfacial shear strength is of special interest. The small diameter of the C-fibres is a big handicap to measure this property directly, e.g. after the "Marshall push-in method". Therefore, only few data can be found in literature about the interfacial shear strength of thin C-fibres embedded in glass or ceramics. In [37] values are given for the interfacial shear strength of 10.2 MPa and in [30] 55 MPa; because no clear values are obtainable the following calculations are made using these two values for all fibre types. The surface energy of Pyrex glass is given in [30] to be 4 J m^{-2} . This value is also taken for the calculations with DURAN glass.

Table IIIa contains values for experimentally determined strains at a maximum matrix strength for the various fibre/glass composites and for the calculated

TABLE IIIa Strains at matrix fracture (at bendover stress), experimental (ϵ_{el}) and theoretical (ϵ_o) based on the model of Aveston, Cooper and Kelly (ACK) and on two values of the interfacial shear strength, τ

| Fibre | ϵ_{el} (%) | ϵ_o ACK, $\tau = 10 \text{ MPa}$ (%) | ϵ_o ACK, $\tau = 55 \text{ MPa}$ (%) |
|-------|------------------------|---|---|
| T300 | 0.40 ± 0.02 | 0.20 | 0.35 |
| T800 | 0.48 ± 0.07 | 0.23 | 0.41 |
| T1000 | 0.46 ± 0.06 | 0.23 | 0.40 |
| M40J | 0.50 ± 0.08 | 0.23 | 0.40 |
| M46J | 0.40 ± 0.03 | 0.24 | 0.42 |
| M55J | 0.38 ± 0.05 | 0.24 | 0.41 |
| M60J | 0.29 ± 0.06 | 0.25 | 0.43 |
| M30 | 0.41 ± 0.04 | 0.21 | 0.37 |
| M40 | 0.48 ± 0.03 | 0.21 | 0.37 |

TABLE IIIb Bendover stresses at matrix fracture; experimental (σ_{bo}) and theoretical (σ_o) based on the model of ACK and on two values of the interfacial shear strength, τ

| Fibre | σ_{bo} (MPa) | σ_o ACK, $\tau = 10 \text{ MPa}$ (%) | σ_o ACK, $\tau = 55 \text{ MPa}$ (%) |
|-------|------------------------|---|---|
| T300 | 554 ± 16 | 274 | 480 |
| T800 | 766 ± 148 | 350 | 623 |
| T1000 | 746 ± 96 | 370 | 644 |
| M40J | 936 ± 152 | 414 | 720 |
| M46J | 876 ± 56 | 506 | 886 |
| M55J | 1060 ± 120 | 653 | 1115 |
| M60J | 848 ± 144 | 695 | 1195 |
| M30 | 646 ± 65 | 321 | 566 |
| M40 | 1020 ± 69 | 441 | 777 |

ones after the ACK model, using the two interfacial strength values. Analogously, Table IIIb shows the measured values at the bendover stress and those calculated by the ACK model and by the calculated stresses from the experimentally determined Young's moduli. Good agreement is found between the experimentally determined and calculated bendover stresses and respective strains, when the large interfacial shear strength values are used for the ACK model calculations. A reduction of the bending stresses should be expected when the axial thermal stresses are regarded, which originate during cooling of the samples from just above the T_g . The fact that the measured bendover stresses in their order of magnitude correspond to the calculated fracture stresses of the matrix leads to the question whether a portion of the axial thermal stresses are reduced by sliding at the fibre-matrix interface during cooling. On the other hand, the possibility exists that crack initiation occurs at considerably lower stresses than in the bending test and cannot therefore be detected. Only the propagation of these cracks is registered, combined with a clear deviation from the linear relation between stress and strain (bendover stress).

The applicability of the ACK model in combination with the large interfacial shear stresses leads to the conclusion that the C-fibres are bonded relatively strongly to the matrix. This is in agreement with the measured large interlaminar shear strength values which frequently show values between 80 and 100 MPa, particularly for the pore-free hm-C-fibre reinforced composites. A further indication for the large interfacial shear strength is the dominance of the C-fibres in the hysteresis-free thermal expansion within the error limit of $\pm 1 \times 10^{-7} \text{ K}^{-1}$ and the low thermal expansion coefficients [38], as well as the lack of pull-out effects in the fibre volume concentration range of the present investigation.

The main bonding mechanism is obviously the mechanical keying at the fibre-matrix interface. The large radial thermal shrinkage of the fibres is compensated for, in this case, by a radial mechanico-thermal extension. This is possible because the radial Young's modulus of the fibres is very low (ca. 15 GPa, producer's data) compared even to that of the glass matrix.

Acknowledgements

The authors are grateful to Drs Pannhorst, Spallek, Beier and Heinz at Schott Glaswerke, Mainz, for discussions and for the slurry materials. The investigations were funded by the German Federal Ministry of Research and Technology (BMFT), project no. 03M1035D9. The authors are responsible for the content of this publication.

References

1. S. M. LEE, in "International encyclopedia of composites", Vol. 2. (VCH Publishers, New York, 1990) p. 315.
2. W. SEMAR and J. EUL, Faserverstärkte Glasverbundkörper. Fortschrittsberichte der Deutschen Keramischen Gesellschaft. Band 3 (1988), Heft 2.

3. Th. KLUG, J. REICHERT and R. BRÜCKNER, *Glastechn. Ber.* **65** (1992) 41.
4. Z. LU, in "Advances in composites tribology", edited by K. Friedrich (Elsevier, Amsterdam, 1992).
5. A. SKOP, M. WOYDT, K.-H. HABIG, Th. KLUG and R. BRÜCKNER, *Wear*, **169** (1993) 243.
6. R. BRÜCKNER and H. HEGELER, in "Advanced composite materials" edited by M. D. Sacks, Symposium, November 1990, Orlando, FL (Ceramic Transactions, Vol. 19 of the Amer. Ceram. Soc., Inc., Westerville, OH, 1991) p. 797.
7. H. BÖDER, D. GÖLDEN, Ph. ROSE and H. WÜRMSEHER, *Z. Werkstoff.* **11** (1980) 275.
8. H. HOLLEK, *Bornträger Verlag Berlin* (1981) 27.
9. E. FITZER and H. JÄGER, *Z. Werkstoff.* **16** (1985) 215.
10. J. A. H. DE PRUNEDA and R. J. MORGAN, *J. Mater. Sci.* **27** (1990) 4776.
11. E. FITZER, H. MÜNCH, D. NIEDER, G. SCHOCH, T. STUMM and R. ZIMMERMANN-CHOPIN, *Hochfeste faserverstärkte Verbundwerkstoffe mit keramischer Matrix. BMFT-Abschlußbericht 1989.*
12. Torayca technical reference manual. Toray Industries, 1989.
13. W. K. TREDWAY and K. M. PREWO, *Carbon* **27**(5) (1989) 717.
14. K. F. ROGERS, L. N. PHILLIPS and D. M. KINGSTON-LEE, *J. Mater. Sci.* **12** (1977) 718.
15. M. ROZPLOCH and W. MARCINIAK, *High Temp-High Press.* **18** (1986) 585.
16. Th. KLUG and R. BRÜCKNER, *Glastechn. Ber.* **65** (1992) 299.
17. W. PANNHORST, M. SPALLEK, R. BRÜCKNER, H. HEGELER, C. REICH, G. GRATHWOHL, B. MEIER and D. SPELMAN, *Ceram. Engng. Sci. Proc.* **11** (7-8) (1990) 947.
18. H. HEGELER and R. BRÜCKNER, *J. Mater. Sci.* **24** (1989) 1191.
19. Th. KLUG and R. BRÜCKNER, *J. Mater. Sci.* (1994).
20. M. ROSENSAFT and G. MARON, *J. Comp. Tech. Res.* **7** (1985) 12.
21. A. W. CHRISTIANSEN, J. LILLEY and J. B. SHORTALL, *Fibre Sci. Technol.* **7** (1974) 1-13.
22. T. A. MICHALSKE and J. R. HELLMANN, *J. Amer. Ceram. Soc.* **71**(9) (1988) 725.
23. J. M. MCKITTRICK, N. S. SRIDHARAN and M. F. AMA-TEU, *Wear* **96** (1984) 285.
24. S. M. BLEAY and V. D. SCOTT, *J. Mater. Sci.* **26** (1991) 2229.
25. D. W. SHIN and K. M. KNOWLES, in Proceedings of the Institute of Mechanical Engineers FRC 90, p. 163.
26. V. GUNAY, P. F. JAMES and J. E. BAILEY, in Proceedings of the International Conference on New Materials and their Applications, University of Warwick, UK, 1990 (Inst. Phys. Conf. Ser. No. 111) p. 217.
27. H. KERN and J. JANCZAK, *Mat.-wiss. und Werkstofftech.* **23** (1992) 54.
28. R. A. J. SAMBELL, D. C. PHILLIPS and D. H. BOWEN, in Proceedings of the International Conference organized by the Plastic Institute, February 1974, p. 105.
29. J. F. BACON and K. M. PREWO, Research on graphite reinforced glass matrix composites. NASA contract report 145245, UTRC 1977.
30. J. AVESTON, G. A. COOPER, and A. KELLY, in Conf. Proc. Nat. Phys. Lab. 1971, p. 15.
31. M. BARSOUM and B. PLOTNICK, Unpublished data.
32. J. AVESTON and A. KELLY, *J. Mater. Sci.* **8** (1973) 352.
33. H. HEGELER and R. BRÜCKNER, *J. Mater. Sci.* **27** (1992) 1901.
34. S-R. LEVITT, *J. Mater. Sci.* **8** (1973) 793.
35. J. J. R. DAVIES, R. F. PRESTON, R. J. LEE and K. N. WALLS, in Proceedings of the International Conference on New Materials and their Applications, University of Warwick, UK, 1990 (Inst. Phys. Conf. Ser. No. 111) p. 197.
36. A. G. EVANS, *Mat. Sci. Engng.* **A107** (1989) 227.
37. D. H. GRANDE, J. F. MANDELL and K. C. C. HONG, *J. Mater. Sci.* **23** (1988) 311.
38. Th. KLUG, V. FLEISCHER and R. BRÜCKNER, *Glastechn. Bes.* **66** (1993) 201.

*Received 2 April 1993
and accepted 3 February 1994*